Title: The *Drosophila* chromodomain protein Kismet activates steroid hormone receptor transcription to govern axon pruning and memory *in vivo*

Authors: Nina K. Latcheva[1, 2], Jennifer M. Viveiros[1], and Daniel R. Marenda[1, 2, 3*]

Addresses: [1]Department of Biology, Drexel University, Philadelphia, PA, and [2]Program in Molecular and Cellular Biology and Genetics, Drexel University College of Medicine, Philadelphia, PA; [3]Department of Neurobiology and Anatomy, Drexel University College of Medicine, Philadelphia, PA

***Correspondence:** Daniel R. Marenda, Department of Biology, Drexel University, 3141 Chestnut St., Philadelphia, PA 19104.
e-mail: daniel.marenda@drexel.edu

Short Title: Epigenetic control of axon pruning

Key Words: *Drosophila*, *kismet*, axon pruning, Ecdysone Receptor, CHARGE Syndrome, CHD7.

Abstract

Axon pruning is critical for the proper synapse elimination required for sculpting precise neural circuits. Though axon pruning has been described in the literature for decades, relatively little is known about the molecular and cellular mechanisms that govern axon pruning *in vivo*. Here, we show that the epigenetic reader Kismet (Kis) binds to cis-regulatory elements of the steroid hormone receptor *Ecdysone Receptor* (*EcR*) gene in *Drosophila* neurons. Kis is required to activate *EcR* transcription at these elements and promote H3K36 di- and tri-methylation. We show that exogenous EcR can rescue axon pruning and memory defects associated with loss of Kis, and that the histone deacetylase inhibitor SAHA can rescue these phenotypes. EcR protein abundance is a cell-autonomous, rate-limiting step required to initiate axon pruning in *Drosophila,* and our data suggests that this step is under epigenetic control.

Running Title

Kismet activates EcR to promote axon pruning *in vivo*

Highlights (bullet points up to 4)

- The chromodomain reader Kismet activates transcription of the steroid hormone receptor *EcR-B1* in the *Drosophila* to initiate developmental axon pruning.
- Kismet promotes H3K36 di- and tri-methylation at the *EcR* locus and upstream cis-regulatory sites.
- Axon pruning and memory defects associated with loss of Kismet are significantly rescued by general HDAC inhibition.

47 **Introduction**

48 The elimination and refinement of synaptic connections is an integral part of normal
49 development in vertebrates and invertebrates alike. Early in the developing nervous system
50 periods of progressive growth result in an overelaboration of synaptic connections onto a
51 target. Inappropriate synapses then need to be eliminated to establish functional
52 organization of the neuronal circuitry [1]. The pruning of these exuberant connections can
53 occur on a small scale, as with dendritic remodeling, or on a large scale such as with axon
54 retraction and degeneration, with each type occurring through distinct molecular
55 mechanisms [2]. Precise control of axon pruning is critical for proper nervous system
56 function, as defects in pruning have been well documented to lead to developmental brain
57 and psychiatric disorders [1]. Despite its vital role, relatively little is known about the
58 mechanisms that govern axon pruning *in vivo*. What is well known about this process is
59 that it requires tight regulation of gene expression in order to execute the necessary
60 signaling pathways in a temporal and tissue specific manner [3,4]. Epigenetic regulation is
61 key to orchestrating precise gene expression programs for many tightly controlled
62 processes in the body. However, its involvement in axon pruning is still unclear.

63 Holometabolous insects provide an attractive model for studying axon pruning as their
64 nervous system undergoes extensive reorganization during metamorphosis [5,6]. In
65 *Drosophila melanogaster* the larval neuronal circuitry is eliminated to make way for adult
66 specific circuitry that governs adult behavior. The most notable changes occur in the
67 learning and memory processing center of the fly brain known as the mushroom bodies
68 (MBs) [7-10]. MB neurons undergo a selective, stereotypical pruning during metamorphosis,
69 which is initiated by the steroid hormone 20-hydroxyecdysone (ecdysone) [3,11,12]. Ecdysone

70 binds to the Ecdysone Receptor (EcR), and translocates to the nucleus to initiate
71 transcription of a subset of regulatory target genes required for axon pruning. MB neurons
72 that undergo remodeling express a particular isoform of the EcR, EcR-B1, which has been
73 shown to be a rate-limiting and cell-autonomous step required for developmental axon
74 pruning [11].

75 Our lab previously identified the chromodomain protein Kismet (Kis) as necessary for
76 proper developmental axon pruning in the *Drosophila* MB neurons [13]. Kis is the
77 *Drosophila* ortholog of the mammalian chromatin ATPase CHD7, a chromatin "reader"
78 that is thought to play a role in chromatin remodeling by binding to methylated histone
79 tails [14]. In humans, heterozygous mutations in *CHD7* cause CHARGE syndrome [15], an
80 autosomal dominant neurodevelopmental disorder.

81 Here, we investigated the role of Kis in the developmental axon pruning of the
82 *Drosophila* MB neurons. We determined that the loss of Kis in the MBs results in pruning
83 defects during metamorphosis, which persist into adulthood and are due to a decrease in
84 transcription of *EcR-B1*. We show that endogenous Kis is enriched at cis-regulatory
85 enhancer sites as well as the transcriptional start site (TSS) of the *EcR* locus. Further, loss
86 of Kis leads to a decrease in the histone marks H3K36me2 and H3K36me3, which have
87 been associated with actively transcribed genes. Adult flies with Kis specifically decreased
88 in the MB neurons display a loss of immediate recall memory, which is rescued by
89 exogenous expression of EcR-B1. Finally, we show that pharmacological intervention via
90 the general histone deacetylase (HDAC) inhibitor suberoylanilide hydroxamic acid
91 (SAHA) can rescue the decrease in *EcR-B1* mRNA, axon pruning, and memory defects
92 associated with decreased Kis in MB neurons. Taken together, these data show that Kis-

93 mediated regulation of *EcR-B1* is required for proper developmental axon pruning *in vivo*
94 by mediating the epigenetic marks H3K36me2 and H3K36me3. These novel findings
95 suggest that the rate−limiting step required to initiate axon pruning (*EcR-B1* expression) is
96 under epigenetic control.
97
98 **Results**
99 **Kismet is required for MB pruning**
100 To characterize the pruning defects previously observed in *kis* mutant MB neurons,
101 we utilized the mosaic analysis with a repressible cell marker (MARCM) system to
102 generate homozygous mutant neuroblast clones tagged with a membrane bound GFP using
103 the *201Y*-Gal-4 driver [13,16-18]. We measured dorsal, medial, and total surface area of the
104 MB lobes in pupal brains 18-22 hours after puparium formation (APF). At this timepoint,
105 the MB lobes are mostly pruned away in control animals (Fig. 1A, 1E). In the null mutant
106 kis^{LM27}, MB clones had significantly larger medial and total lobe surface areas compared
107 to control MB clones (Figs. 1A, 1B, 1E). MB clones expressing the wild-type Kis-L protein
108 in the kis^{LM27} mutant background showed a significant reduction of the medial and total
109 lobe areas back to control levels (Figs. 1D, 1E). Overexpression of Kis-L alone did not
110 have an effect on lobe surface area (Figs. 1C, 1E). In addition to MARCM analysis, we
111 utilized RNA interference (RNAi) mediated knockdown of Kis with two separate
112 previously validated RNAi constructs to verify the pruning defects [13]. Pan-neural
113 knockdown of Kis using the *elav*-Gal-4 driver showed a significant increase in the medial
114 and total lobe areas compared to outcross controls (Supplemental Figure 1). Similar to the
115 MARCM analysis, pan-neural expression of Kis-L in the knockdown genetic backgrounds

116 was able to significantly rescue the medial and total surface area levels (Supplemental
117 Figure 1). Taken together, these data show that Kis is required for the developmental axon
118 pruning of MB neurons during metamorphosis.
119
120 **Kismet binds EcR and activates EcR transcription**
121 Expression of the steroid hormone receptor EcR-B1 is the first step in the
122 developmental axon pruning of the MB neurons, and loss of EcR-B1 function produces
123 defects in pruning similar to what we observe in decreased Kis function [11]. Therefore, we
124 sought to determine if Kis affects levels of EcR-B1. RNAi knockdown of Kis in MB
125 neurons *in vivo* showed a significant decrease in EcR-B1 immunofluorescence compared
126 to control MBs (Figs. 1F-1K, Fig. 1R). In support of this, mRNA levels of EcR-B1 were
127 significantly reduced in pupae with decreased Kis as well (Fig. 1S). Finally, we wanted to
128 determine if addition of exogenous Kis-L in Kis knockdown MBs could rescue the loss of
129 EcR-B1 expression. We found that replacement of Kis-L protein did successfully rescue
130 both decreased EcR-B1 mRNA and protein expression in these neurons (Figs. 1L-1S).
131 Taken together, these data suggest that Kis is required to promote EcR-B1 expression
132 within MB neurons.
133 Given that Kis is an epigenetic chromatin reader, we theorized that it may be
134 affecting EcR-B1 mRNA and protein levels by promoting transcription. To test this, we
135 performed chromatin immunoprecipitation (ChIP) followed by qPCR to analyze Kis
136 occupancy at previously published cis-regulatory elements of the *EcR* locus as well as the
137 *EcR* TSS (Fig. 2A) [19]. We utilized a Kis-eGFP protein trap animal previously described to
138 express a eGFP tagged version of the Kis protein [20] [21]. Importantly, this animal shows

139 normal localization and function of Kis, and we have shown that our RNAi reagents can
140 successfully knockdown the eGFP tagged Kis protein and *kis* mRNA (Supplemental Figure
141 2) [20]. We utilized the *forkhead* (*fkh*) TSS as a positive control, as it was previously reported
142 to be bound by endogenous Kis [22]. Additionally, we used the *dynamin* homolog *shibire*
143 (*shi*) as a negative control, as we had previously shown via microarray analysis that loss of
144 Kis did not have any significant effect on *shi* expression [20]. We verified that Kis was not
145 enriched at the *shi* promoter region (Fig. 2A), and that knockdown of Kis did not have any
146 significant effect on Kis abundance at the *shi* promoter (Fig. 2A). In contrast, wild-type
147 control brains showed enrichment of Kis at the two previously reported *EcR* cis-regulatory
148 elements (*EcR.1* and *EcR.2*) as well as the *EcR* and *fkh* TSS (Fig. 2A). Finally, we observed
149 a significant decrease in Kis enrichment at the *fkh* TSS, *EcR.1*, *EcR.2*, and *EcR* TSS sites
150 when Kis was knocked down, confirming specificity of Kis binding at these sites (Fig. 2A).
151 These results suggest that Kis binds to known cis-regulatory sites and the TSS of the *EcR*
152 locus in *Drosophila* larval brains.

153 To determine if Kis can control transcriptional output from these sites, we utilized
154 an EcR transcriptional reporter (*EcR.1*-Gal-4, described in [23,24]). This reporter drives the
155 expression of the exogenous Gal-4 protein from the *EcR.1* cis-regulatory element that is
156 partially responsible for the expression of *EcR-B1* in MB neurons [19] . Using this reporter,
157 we determined the levels of Gal-4 mRNA and protein in wild-type control MBs and Kis
158 knockdown MBs. We observed a significant decrease in both Gal-4 mRNA and protein
159 levels from this reporter in Kis knockdown animals compared to controls (Figs. 2C-G).
160 Taken together, these data suggest that Kis protein can bind to *EcR* cis-regulatory elements

161 and the *EcR* TSS to promote transcriptional activation and increase EcR-B1 expression in
162 the *Drosophila* nervous system.
163
164 **Kismet promotes H3K36me2 and H3K36me3**
165 One mechanism by which chromatin remodeling proteins promote transcriptional
166 activation is by mobilizing nucleosomes and allowing transcriptional machinery access to
167 enhancer sites and promoters of target genes [25]. Given Kis's homology to CHD7 and its
168 conserved ATPase domain, we hypothesized that Kis may be removing nucleosomes from
169 the *EcR* locus to allow access to the transcriptional machinery. To test this possibility, we
170 immunoprecipitated total histone 3 (H3) protein at the *EcR* locus in control and Kis
171 knockdown brains. However, we found no significant difference between these conditions
172 at each of the cis-regulatory loci we analyzed (Fig. 2B). To verify this, we performed an
173 MNase protection assay. Consistent with our total H3 analysis, we saw no change in the
174 digestion of chromatin upon Kis knockdown (Supplemental Figure 3). Taken together,
175 these data suggest that Kis is not affecting the movement of nucleosomes as a mechanism
176 to promote transcription at the *EcR* locus.
177 Another way chromatin readers can affect gene expression is by altering the histone
178 modifications present at relevant genomic loci [25], and Kis has been shown to affect histone
179 modifications previously [22]. We began by analyzing H3K4 methylation states at *EcR* loci
180 in control and Kis knockdown animals, as it is the type of methylation most commonly
181 associated with actively transcribed genes. ChIP-qPCR analysis showed no change in all
182 types of H3K4 methylation levels upon Kis knockdown at these loci (Supplemental Figs.
183 4A-C). We next analyzed H3K27 trimethylation, as this modification is often associated

184 with gene repression. We did not observe any significant change in H3K27 trimethylation
185 upon Kis knockdown at any of the loci examined (Supplemental Fig. 4D). Taken together,
186 these data suggest that alteration of H3K4 methylation or H3K27 trimethylation is not part
187 of the mechanism by which Kis controls *EcR* transcription.

188 Previous studies demonstrated a global decrease in H3K36 di- and tri-methylation
189 upon Kis loss in *Drosophila* salivary gland polytene chromosomes [26]. In *Drosophila*, this
190 type of modification is usually associated with actively transcribed genes [26-28]. We
191 therefore sought to determine if the same effect on H3K36 methylation was present in the
192 *Drosophila* nervous system upon pan-neural knockdown of Kis protein. We observed that
193 H3K36me2 was significantly decreased at all the *EcR* cis-regulatory sites, as well as at the
194 *fkh* positive control, in Kis knockdown brains compared to controls (Fig. 2H). Additionally,
195 H3K36me3 was also significantly decreased at the *EcR* and *fkh* TSS (Fig. 2I). Importantly,
196 this decrease in H3K36 methylation was not global, as there was no significant change with
197 either H3K36 di- or tri-methylation at the *shi* promoter which is not bound by Kis (Figs.
198 2A, 2H-I). Also, given that H3K36me2 is the substrate for the tri-methylated form, it is
199 likely that the decrease in H3K36me3 is due to the decrease in H3K36me2. Combined,
200 these results suggest Kis affects transcription at the *EcR* locus by promoting the active
201 H3K36 di- and tri-methylation histone marks.

202

203 **EcR-B1 rescues axon pruning defects**

204 EcR-B1 is well documented to be a key player in initiating the axon pruning
205 cascade in MB neurons [4,11]. Given that we have shown Kis acts to promote transcription of
206 *EcR-B1* in MB neurons, we sought to determine if we could rescue the pruning defects we

207 observe is Kis mutants by expression of exogenous EcR-B1. Utilizing the MARCM
208 system, we expressed exogenous EcR-B1 protein within *kis*^{LM27} mutant MB clones (Fig.
209 3). We observed that exogenous expression of EcR-B1 significantly reduced the abnormal
210 pruning observed in *kis*^{LM27} mutant MB clones (Figs. 3B, 3D, 3E). We also observed a
211 significant reduction in pruning defects when exogenous EcR-B1 was pan-neurally co-
212 expressed with Kis RNAi constructs (Supplemental Fig. 5). Interestingly, EcR-B1
213 overexpression alone, as well as EcR-B1 expression in Kis loss of function backgrounds,
214 produced smaller surface areas in the dorsal and total lobes compared to outcross controls
215 (Figs. 3A, 3C, 3E-3F). This is consistent with Kis functioning upstream of EcR-B1 in the
216 pruning process, as well as with EcR-B1 being the rate-limiting factor for pruning. Taken
217 together, these data suggest that Kis mediates axon pruning in MB neurons by
218 transcriptionally activating *EcR-B1*, thereby controlling EcR-B1 protein levels.

219 Pruning defects observed during metamorphosis may simply reflect a delay in
220 normal pruning. Therefore, to determine that homozygous MARCM *kis*^{LM27} mutant clones
221 indeed have defective developmental pruning, as opposed to having delayed pruning, we
222 sought to determine if the unpruned axons persisted into adulthood. We generated
223 MARCM clones with homozygous *kis*^{LM27} MBs as previously described and aged the
224 adults for 5 days after eclosion. We then immunostained the adult brains with anti-FASII,
225 a transmembrane cell adhesion protein, which is differentially expressed in the separate
226 populations of MB neurons [29,30]. FASII expression is lowest in the early born gamma
227 neurons and highest in the late born alpha/beta neurons; therefore, the appearance of GFP
228 labeled MARCM axons in the dorsal lobe that are weakly or unstained for FASII would
229 constitute aberrant unpruned axons that persisted into adulthood [29]. Compared to control

230 MBs, *kis*^{LM27} MARCM clones had significantly more weakly-stained and/or unstained
231 FASII GFP-positive axons outside the dorsal lobe bundle, indicating that pruning is in fact
232 prevented and not delayed in this mutant (Figs. 3F-3K, 3R). Given that exogenous
233 expression of EcR-B1 in the *kis*^{LM27} MARCM background rescued the pruning defects at
234 the pupal stage, we tested whether the rescue effects of exogenous EcR-B1 provided at the
235 pupal stage also persisted into adulthood. We observed that expression of EcR-B1 in *kis*^{LM27}
236 mutant MARCM clones showed significantly fewer GFP-positive axons outside the dorsal
237 lobe in adult MB axons, while expression of EcR-B1 alone had no effect (Figs. 3L-3Q,
238 3R). Collectively, these data suggest that the defective pruning observed during
239 metamorphosis in *kis* loss-of-function MB neurons persists into adulthood.
240
241 **EcR-B1 rescues memory defects**
242 Previous studies from our lab showed that reduction of Kis levels in MB neurons
243 produced significant defects in immediate recall memory [13]. Since loss of Kis leads to
244 pruning defects that persist into adulthood, and exogenous EcR-B1 expression is able to
245 rescue the defects, we were interested in determining if exogenous expression of EcR-B1
246 could also rescue the memory defect associated with loss of Kis function as well. We
247 utilized the conditioned courtship suppression assay which takes advantage of the innate
248 courting behaviors carried out by male *Drosophila* in response to multimodal signals
249 transduced by females [31-33]. Wild-type males will decrease their rate of courting during
250 training when exposed to an unresponsive female, and continue to court at lower rates even
251 with subsequent receptive females for an average of 1-3 hours after exposure [31-33]. We
252 utilized RNAi to knockdown Kis in MB neurons using the *OK107*-Gal4 driver.

253 Importantly, expression of the Gal4 alone, or Gal4-mediated expression of exogenous EcR-
254 B1 did not produce any learning (Fig. 4A) or memory (Fig. 4B) defects. We observed that
255 males with decreased Kis protein displayed intact learning, as evident by the significant
256 decrease in courtship from the initial to final stages of exposure to an unresponsive female
257 (Fig. 4C). Similarly, males with both decreased Kis and exogenously expressed EcR-B1
258 also had intact learning (Fig. 4C). However, males with decreased Kis showed abnormal
259 memory (Fig. 4D), as these males had rates of courtship that were not significantly different
260 than sham males, which did not receive exposure to an unreceptive female. In contrast,
261 males with both decreased Kis and exogenously expressed EcR-B1 showed significantly
262 reduced courtship in trained males compared to sham males, indicative of intact immediate
263 recall memory (Fig. 4D). Taken together, these data suggest that the memory defects
264 associated with loss of Kis in the MB neurons are due to decreased EcR-B1 levels.
265
266 **SAHA rescues Kis defects**
267 Recently, our lab showed that pharmacological inhibition of HDACs can rescue
268 multiple defects associated with loss of Kis at the neuromuscular junction [34]. HDAC
269 inhibition (HDACi) did not significantly affect *kis* mRNA levels [34], so we hypothesized
270 that rescue may be due to effect on target genes. To further examine this hypothesis, we
271 tested whether HDACi treatment could rescue the decreased EcR-B1 levels, pruning, and
272 memory defects observed in Kis knockdown. We observed that treatment of Kis
273 knockdown animals with SAHA significantly increased *EcR-B1* mRNA levels compared
274 to dimethyl sulfoxide (DMSO) treated controls (Fig. 5S). SAHA treatment alone had no
275 significant impact on axon pruning in either pupal or adult MBs (Figs. 5E, 5R). However,

276 we observed that SAHA treatment significantly decreased the number of unpruned axons
277 in both pupal and adult brains in Kis loss-of-function MB neurons (Figs. 5E, 5R). Finally,
278 SAHA treatment itself did not have an adverse effect on learning or memory in controls
279 (Figs. 6A-6B) and was able to significantly rescue the immediate recall defect in Kis
280 knockdown animals compared to DMSO treatment alone (Figs. 6C-6D). Taken together,
281 these results show that HDACi treatment significantly rescues multiple defects associated
282 with Kis loss-of-function.
283
284 **Discussion**
285 Axon pruning and elimination are critical steps to establishing and refining neural
286 circuitry. However, relatively little is known about the molecular details that control
287 developmental axon pruning. Here we begin to unravel the epigenetic mechanisms
288 essential for initiating developmental axon pruning *in vivo*. We show that the chromatin
289 reader Kis activates transcription of *EcR-B1* in the *Drosophila* MBs and promotes
290 methylation of H3K36 at cis-regulatory sites and the TSS of *EcR-B1*. We show that proper
291 regulation of EcR-B1 by Kis is required for developmental pruning and immediate recall
292 memory in adults. Finally, we show that the general HDACi SAHA can increase *EcR-B1*
293 levels in animals with decreased Kis and rescue the pruning and memory defects. This is
294 the first study demonstrating that the essential rate-limiting step in developmental axon
295 pruning, EcR-B1 expression, is under epigenetic control. Few studies have hinted at an
296 epigenetic mechanism of EcR activation. The *Drosophila* Set2 K36 histone methyl
297 transferase (HMT) was shown to genetically interact with the EcR signaling pathway and
298 positively regulate expression of EcR target genes [27]. However, as dSet2 is required for

299 general transcriptional elongation, this may be a non-specific effect of dSet2 function.
300 Nonetheless, this implicates H3K36 methylation as an important factor in EcR expression.
301 While Kis does not appear to affect expression of dSet2, Ash1 or dMes-4 (data not shown),
302 it might be acting to recruit the HMTs to relevant target genes. To this effect, Kis was
303 previously shown to increase the global association of Ash1 on polytene chromosomes
304 [26,35]. While other studies with Kis have implied a role for the chromatin reader in
305 transcriptional elongation [36], we demonstrate a selectivity for Kis binding and Kis-
306 mediated elevation of H3K36 methylation as no significant changes were observed at the
307 *shi* promoter in Kis knockdown animals. Further work needs to be done to tease apart the
308 relationship between Kis, H3K36 methylation, and any HMTs responsible for this
309 modification in EcR regulation.

310 Much work has been done to understand the crosstalk between different histone
311 modifications and their cumulative outcome on transcription. For example, H3K36me2
312 was reported to specifically increase H4K16 acetylation, a modification most well-known
313 for its role in decondensation of chromatin structure [37,38]. Additionally, this type of
314 acetylation directly influences transcription by positively regulating chromatin
315 accessibility to non-histone proteins [39]. It is therefore plausible that Kis might be affecting
316 transcriptional output by promoting H4K16 acetylation via H3K36me2 crosstalk. This may
317 explain why HDAC inhibition with SAHA, seemingly unrelated to histone methylation, is
318 able to restore *EcR-B1* mRNA levels due to loss of Kis and rescue pruning and memory
319 defects. Furthermore, SAHA treatment has been previously shown to increase H4K16ac
320 and ultimately increase transcriptional output in cancer cells [40]. Further work is essential
321 to building a complete understanding of the integration of extrinsic and intrinsic cues that

322 control transcriptional regulation. This is fundamental to unraveling the mechanisms that
323 underlie the refinement of neural circuits.
324
325
326
327
328
329
330
331
332
333
334
335
336
337
338
339
340
341
342
343
344

345 **Figure 1**

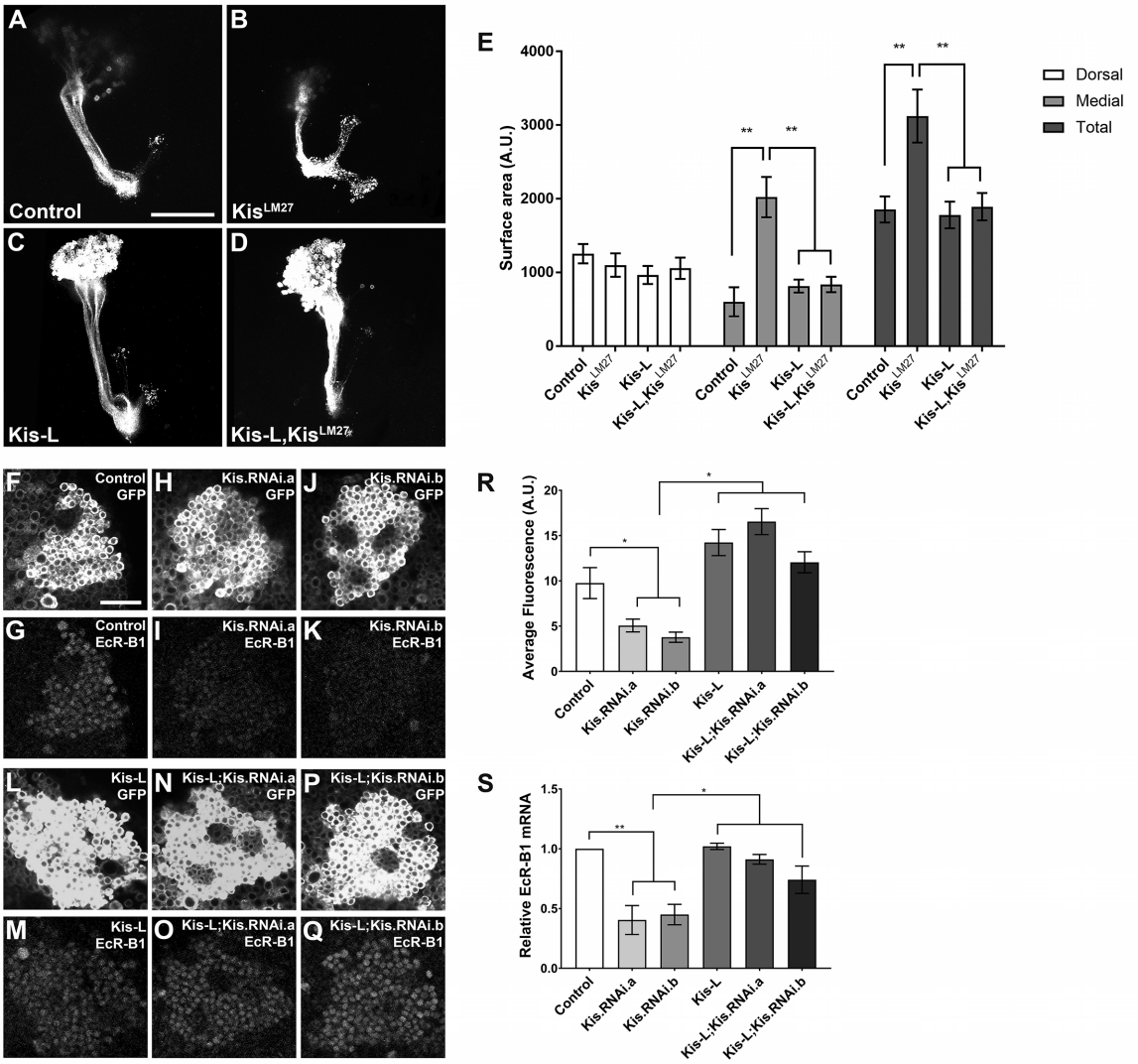

346

347 **Figure 1. Kis is required for axon pruning and EcR expression.** (A-D) Representative
348 images of MARCM generated MB clones expressing membrane bound GFP using the
349 *201Y*-Gal-4 driver 18-22 hours APF. (E) Quantification of dorsal, medial, and total MB
350 lobe surface areas in MARCM animals (n = 8-12). (F-Q) Representative *elav*-Gal-4 driven
351 control, knockdown, overexpression, and rescue pupal brains expressing membrane bound
352 GFP or stained with α-EcR-B1, as indicated. (R) Quantification of fluorescent intensity of
353 EcR-B1 in *elav*-Gal-4 driven pupae (n = 9-12). (S) *EcR-B1* mRNA levels in pupal brains
354 of *elav*-Gal-4 driven animals analyzed by RT-qPCR (n = 3-4). Scale is 10 μm in (A) and
355 20 μm in (F).
356
357
358
359
360

361 **Figure 2**

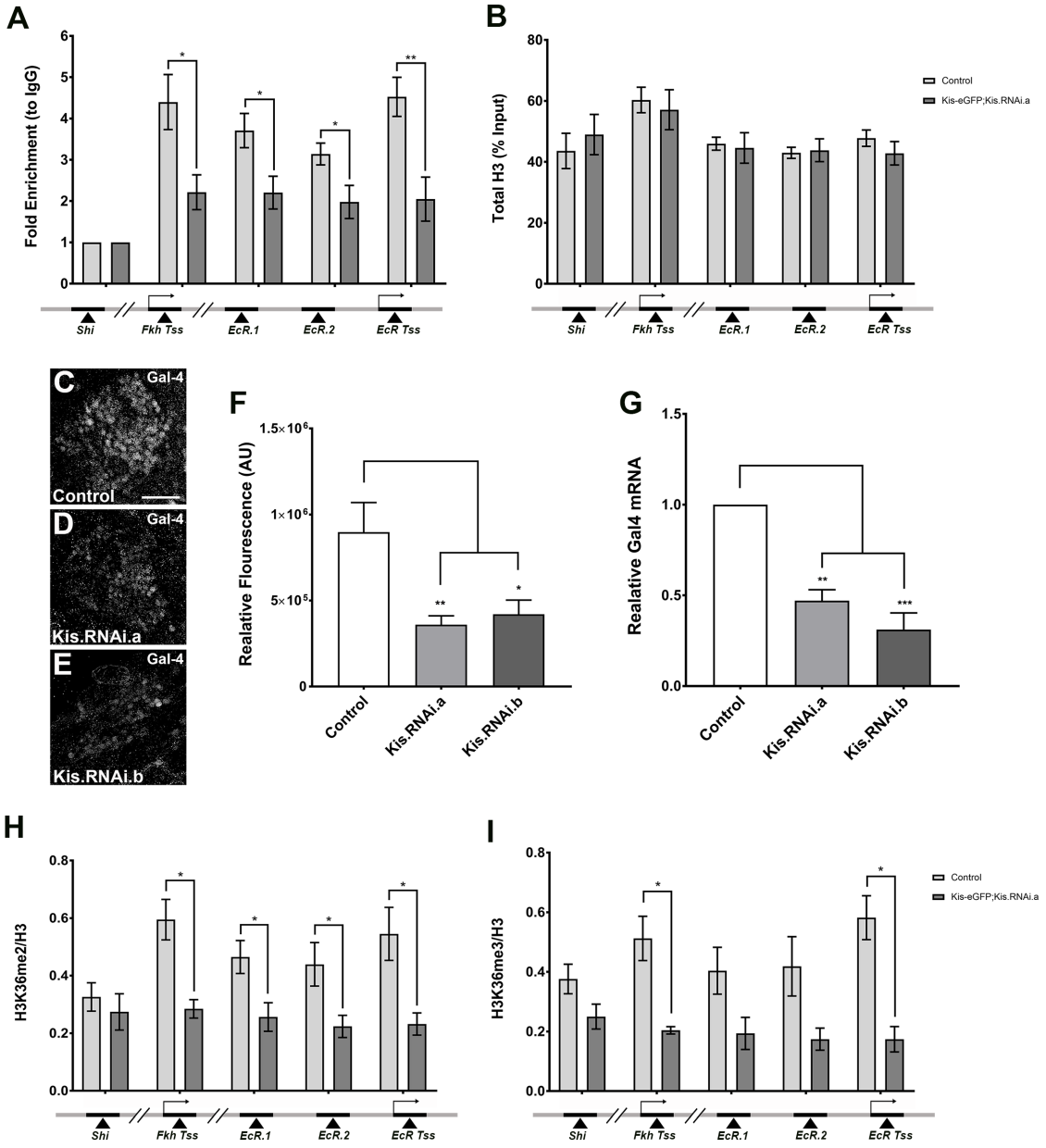

362

363 **Figure 2. Kis binds to EcR loci promoting EcR-B1 transcription and H3K36**
364 **methylation.** (A) ChIP-qPCR analysis using chromatin isolated from 3rd instar larval
365 brains. Kis enrichment at the *EcR* TSS and enhancer sites, the *fkh* TSS, and the *shi*
366 promoter site (n = 4-5). (B) Total H3 as a percentage of the input DNA was determined
367 by qPCR at the previously noted genomic loci (n = 6). (C-E) Representative images of
368 control and knockdown *EcR.1*-Gal-4 driven pupal brains stained with α-Gal-4. (F)
369 Quantification of fluorescent intensity of α-Gal-4 (n = 10). (G) *Gal-4* mRNA levels of
370 *EcR.1*-Gal-4 driven animals analyzed by RT-qPCR (n = 3). (H, I) ChIP-qPCR analysis of

371 H3K36me2 and H3K36me3 abundance relative to total H3 at the above mentioned
372 genomic loci, respectively (n = 3). Scale is 20 μm in (C).
373
374

375 **Figure 3.**

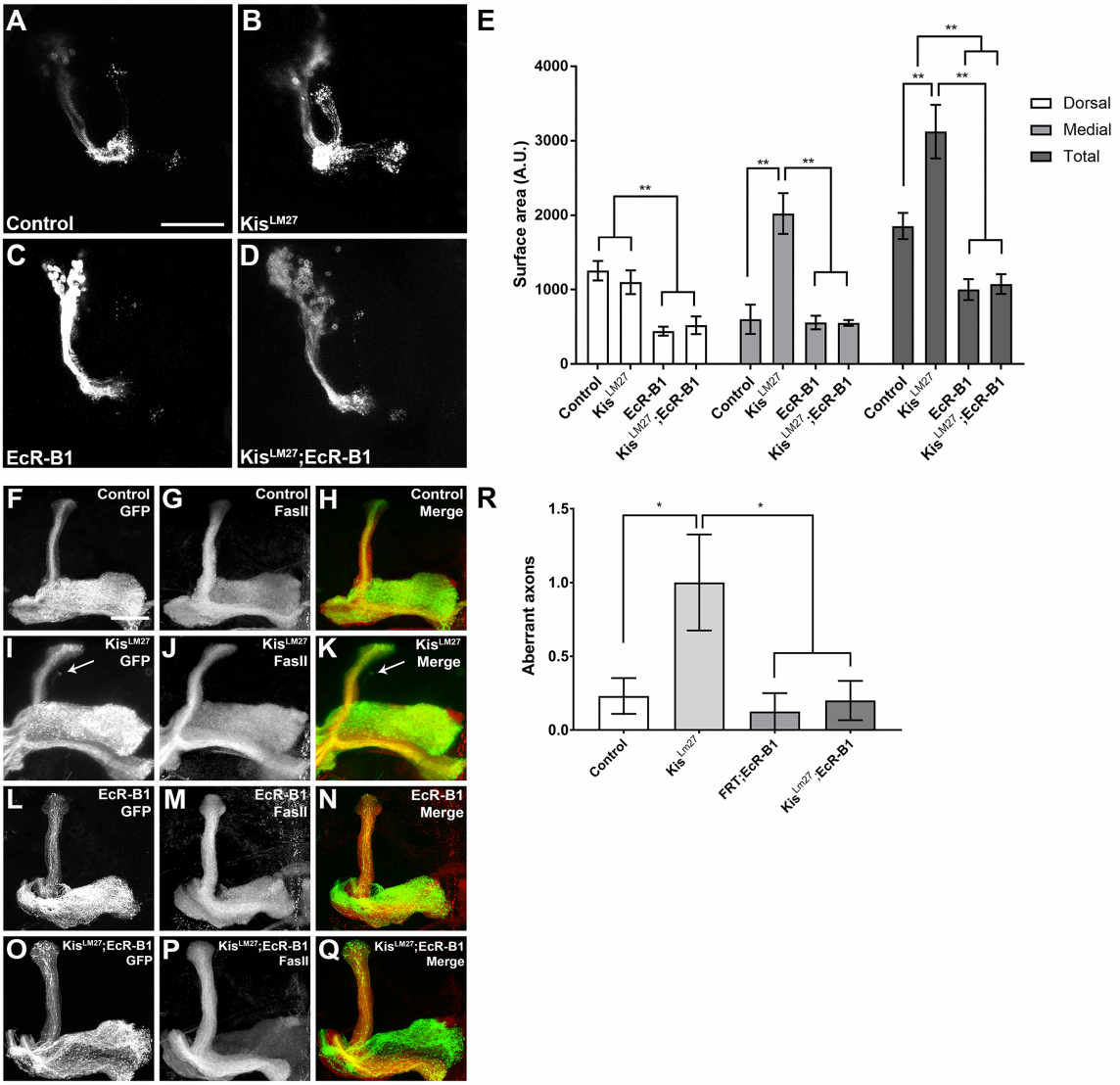

376

377 **Figure 3. Exogenous EcR-B1 rescues defective axon pruning associated with loss of**
378 **Kis.** (A-D) Representative images of MARCM generated MB clones expressing
379 membrane bound GFP using the *201Y*-Gal-4 driver 18-22 hours APF. (E) Quantification
380 of dorsal, medial, and total MB lobe surface areas in MARCM animals (n = 10-12). (F-
381 Q) Representative adult MARCM generated MB clones expressing membrane bound
382 GFP or stained with α-FasII, as indicated. (R) Quantification of aberrant axons in MBs (n
383 = 10). Scale is 10 μm in (A) and 20 μm in (F).

384

385 **Figure 4**

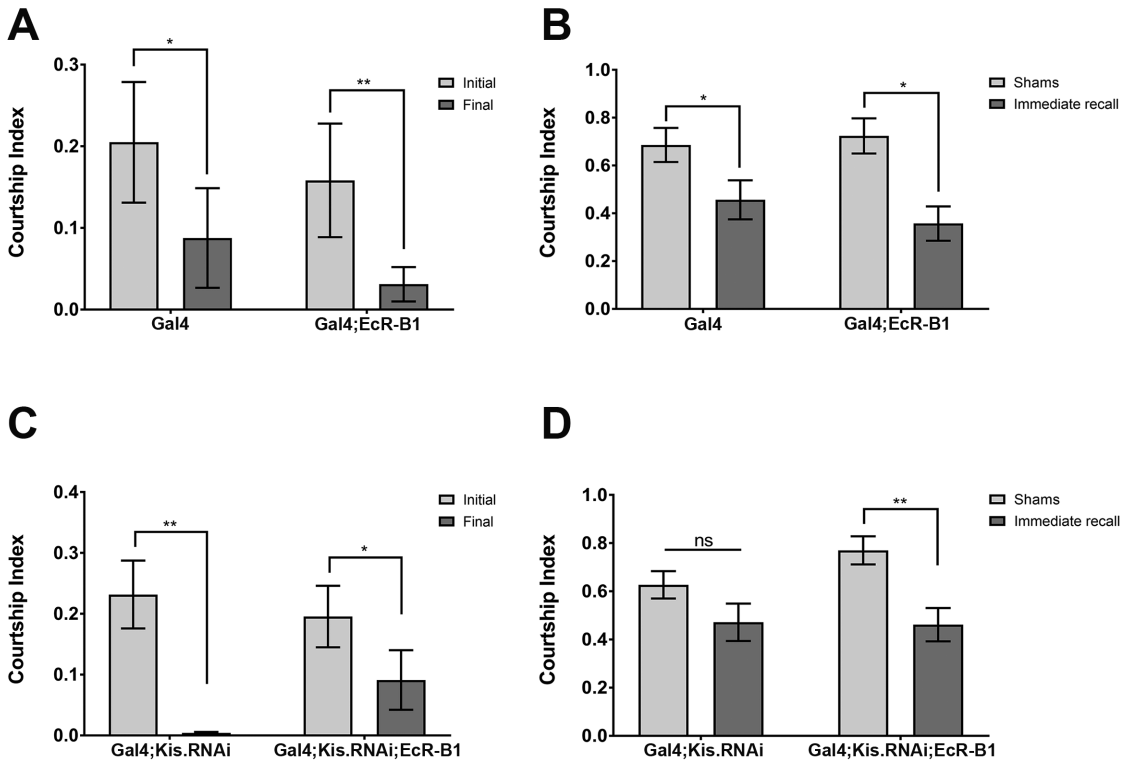

386

387 **Figure 4. Ectopic EcR-B1 expression rescues memory defects rescued in Kis**
388 **knockdown MBs.** (A, C) Change in courtship index of *OK107*-Gal-4 driven males
389 during the initial (light grey) and final (dark grey) 10 minutes was assessed (n = 20-25).
390 (B, D) Immediate recall of trained *OK107*-Gal-4 driven males was assessed and
391 compared to genetically identical sham trained males (n = 20-25).
392

393

394

395

396

397

398

399

400 **Figure 5.**

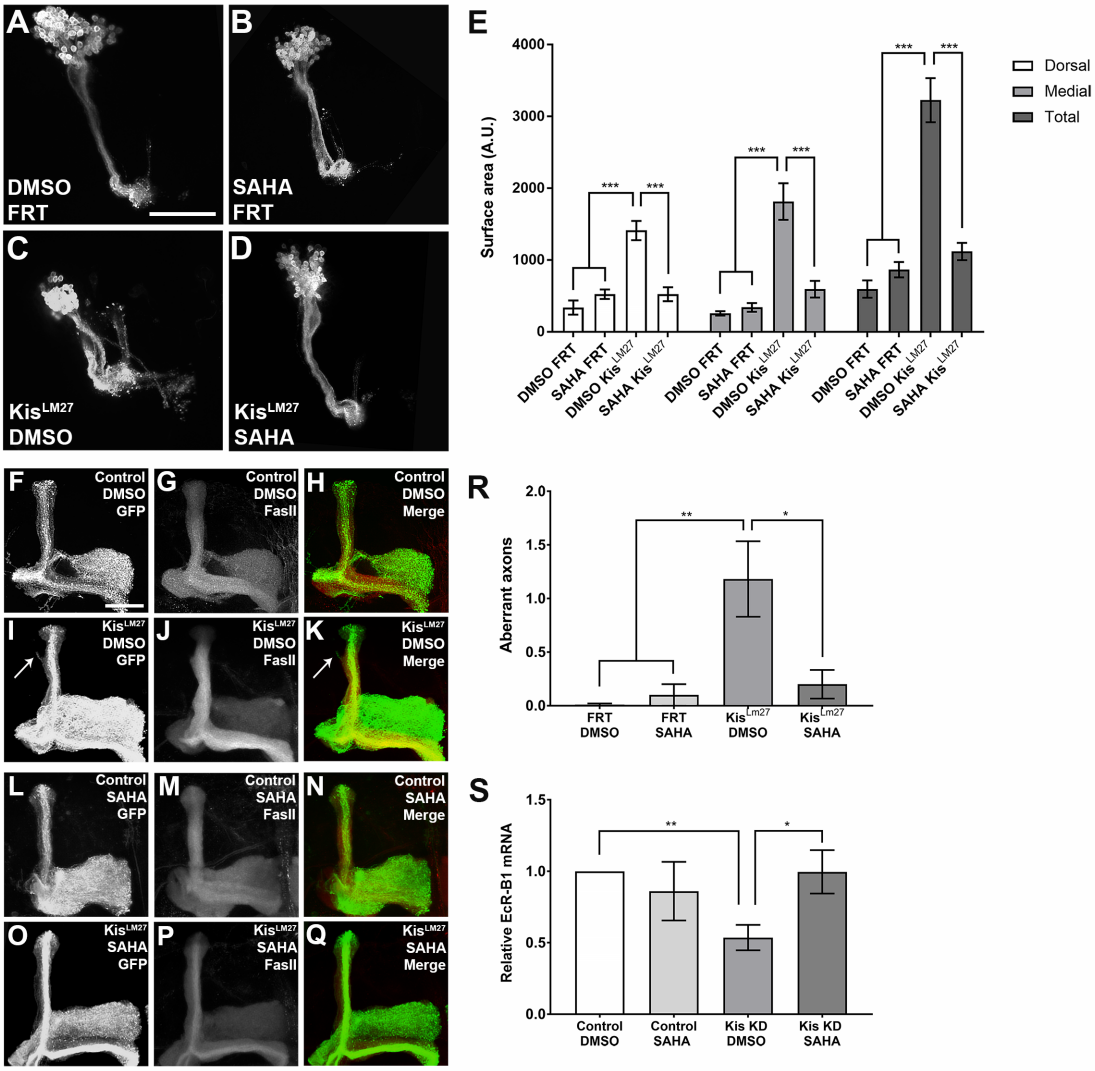

401

402 **Figure 5. HDAC inhibition rescues defective axon pruning and EcR-B1 expression**
403 **in loss of Kis animals.** (A-D) Representative images of DMSO or SAHA treated
404 MARCM generated MB clones expressing GFP using the *201Y*-Gal-4 driver 18-22 hours
405 APF. (E) Quantification of dorsal, medial, and total MB lobe surface areas in DMSO or
406 SAHA treated MARCM animals (n = 10-12). (F-Q) Representative DMSO or SAHA
407 treated adult MARCM generated MB clones expressing membrane bound GFP or stained
408 with α-FasII, as indicated. (R) Quantification of aberrant axons in MBs of flies treated
409 with DMSO or SAHA (n = 10-12). (S) *EcR-B1* mRNA levels in brains of DMSO or
410 SAHA treated *elav*-Gal-4 driven pupae analyzed by RT-qPCR (n = 3-4). Scale is 10 μm
411 in (A) and 20 μm in (F).
412

413

414 **Figure 6.**

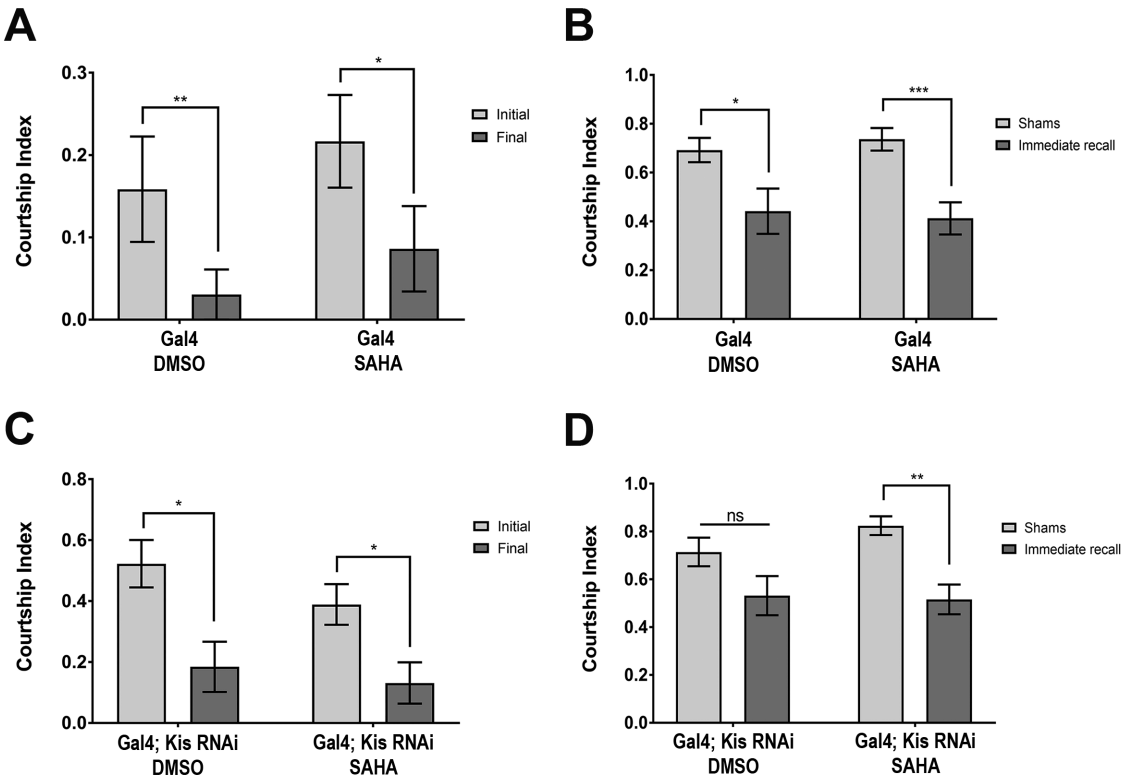

415

416 **Figure 6. SAHA treatment rescues immediate recall defects rescued by in Kis**
417 **knockdown animals.** (A, C) Change in courtship index of DMSO or SAHA treated
418 *OK107*-Gal-4 driven males during the initial (light grey) and final (dark grey) 10 minutes
419 was assessed (n = 20-25). (B, D) Immediate recall of DMSO or SAHA treated trained
420 *OK107*-Gal-4 driven males assessed and compared to genetically identical and treated
421 sham trained males (n = 20-25).
422
423

424

425

426

427

428

429

430

431 **Supplemental Figure 1**

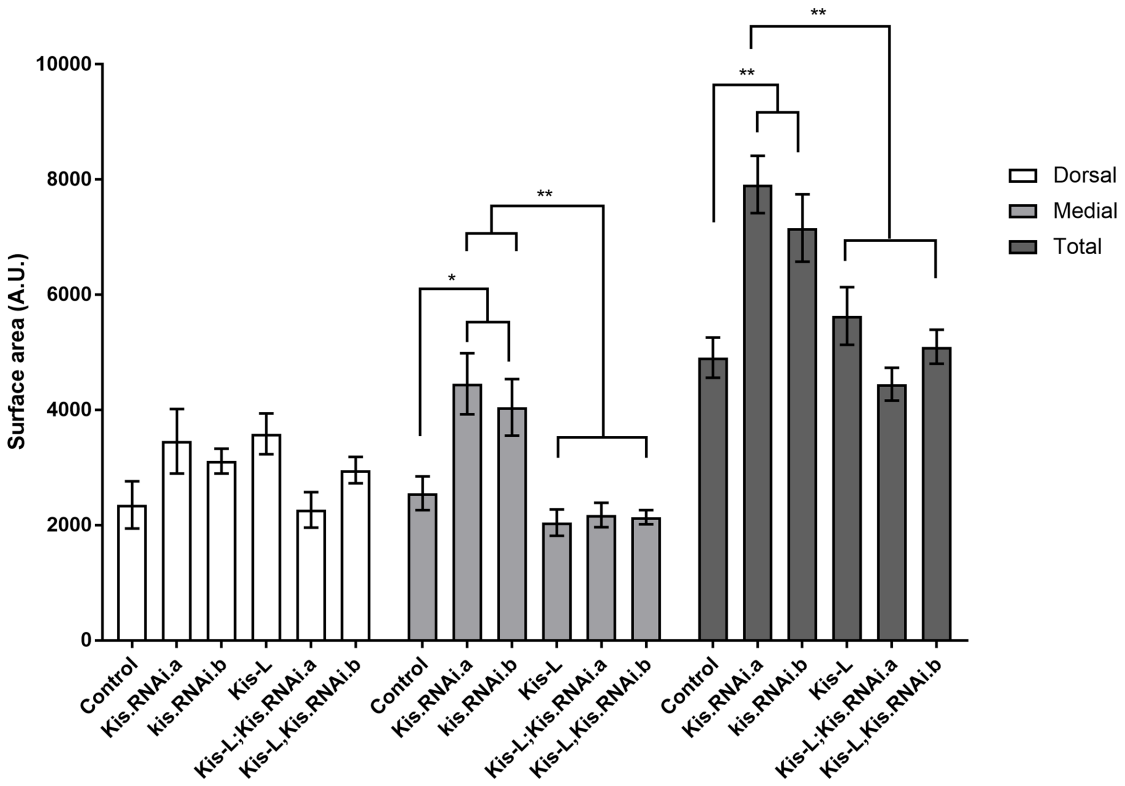

432

433 **Supplemental Figure 1. Kis is required for axon pruning in Kis knockdown pupae.**
434 Quantification of dorsal, medial, and total MB lobe surface areas in *elav*-Gal-4, mCD8-
435 GFP driven pupal brains stained with α-EcR-B1 (n = 10).
436

437

438

439

440

441

442

443

444

445 **Supplemental Figure 2.**

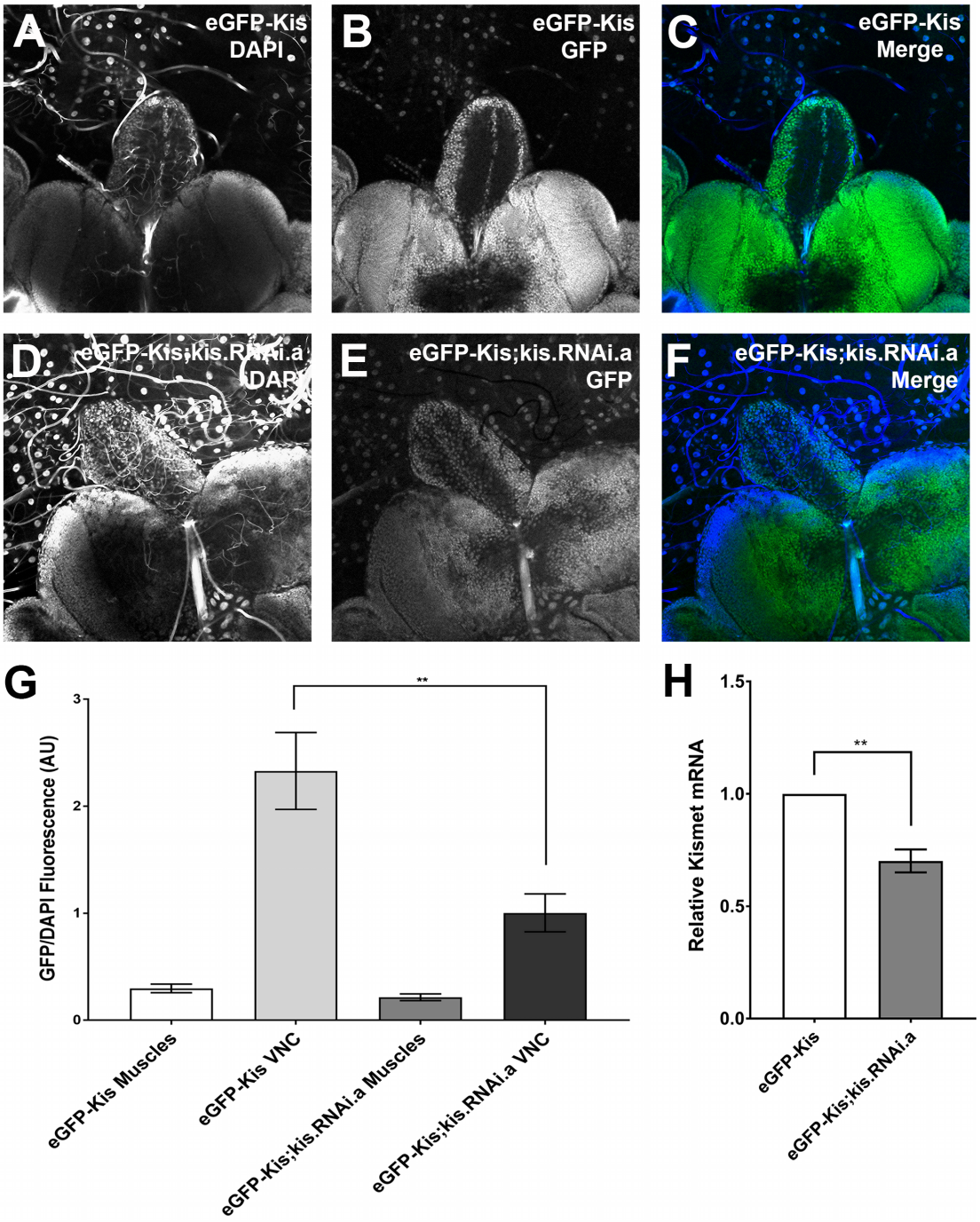

446

447 **Supplemental Figure 2. Kis-eGFP is knocked down by Kis.RNAi.a.** (A-F)
448 Representative images of Kis-eGFP and *elav*-Gal-4 driven knockdown 3rd instar larval
449 brains stained with DAPI. (G) Quantification of GFP fluorescence intensity compared to
450 that of DAPI (n = 9-12). (H) *Kis* mRNA levels in 3rd instar larval brains of *elav*-Gal-4
451 driven control and knockdown analyzed by RT-qPCR (n = 4).

452 **Supplemental Figure 3.**

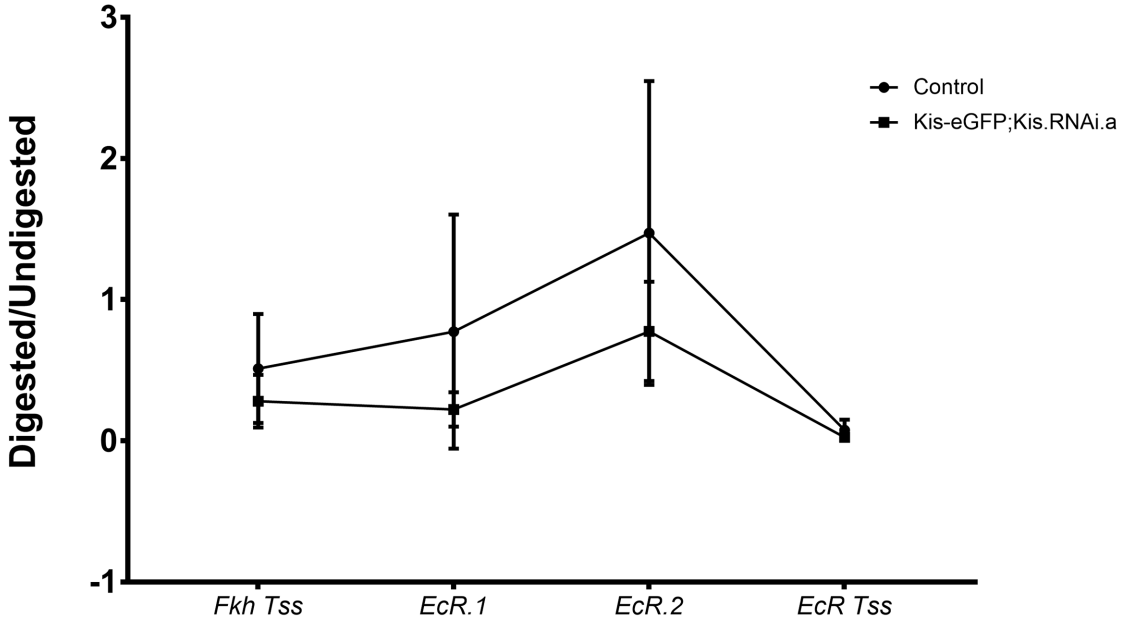

453

454

455 **Supplemental Figure 3. Kis does not alter DNA protection at *EcR* loci.** Quantification
456 of MNase protection assay followed by qPCR at the *EcR* TSS, EcR enhancer sites, and
457 the *fkh* TSS (n = 3).
458

459

460

461

462

463

464

465

466

467

468 **Supplemental Figure 4.**

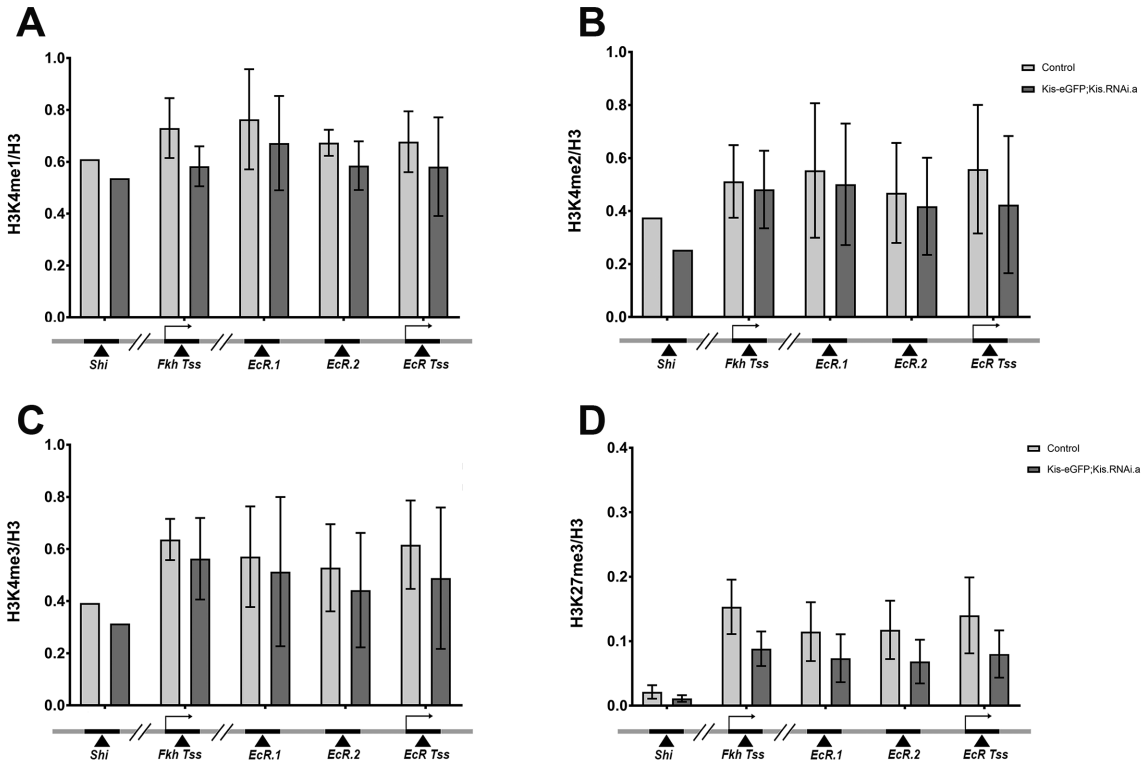

469

470 **Supplemental Figure 4. Kis does not alter H3K4 or H3K27 methylation at *EcR* loci.**
471 (A-D) qPCR analysis H3K4me1, H3K4me2, H3K4me3, H3K27me3 abundance at the
472 *EcR* TSS and enhancer sites, the *fkh* TSS, and the *shi* promoter site, respectively (n = 2-
473 4).
474

475

476

477

478

479

480

481

482

483 **Supplemental Figure 5.**

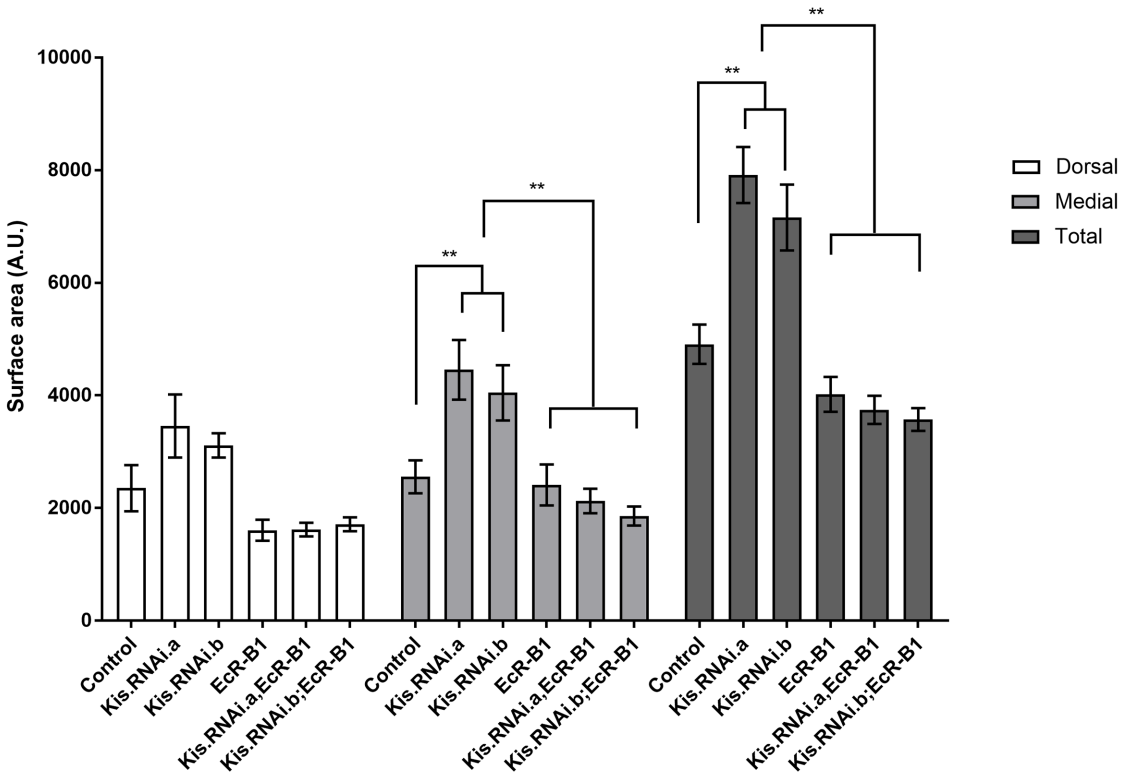

484

485 Supplemental Figure 5. **Exogenous EcR-B1 rescues defective axon pruning in Kis**
486 **knockdown pupae.** Quantification of dorsal, medial, and total MB lobe surface areas in
487 e*lav*-Gal-4, mCD8-GFP driven pupae (n = 10).
488

489

490

491

492

493

494

495

496

497

498 **Methods**

499 Drosophila stocks and genetics

500 Unless otherwise noted, all crosses were carried out at 25 °C in a 12:12 light:dark
501 cycle at 60% humidity on standard cornmeal-molasses-agar medium. BL numbers refer to
502 Bloomington Stock Center (BSC) stock numbers
503 (http://flystocks.bio.indiana.edu/bloomhome.htm). VDRC numbers refer to the Vienna
504 Drosophila Resource Center stock numbers (http://stockcenter.vdrc.at/control/main). To
505 drive the expression of transgenes in Drosophila, the Gal-4/UAS bipartite system was used
506 as previously described [41]. All Gal-4 stocks (*elav*-Gal-4 (BL #458), *elav*-Gal-4,mCD8-GFP
507 (BL #5146), (*OK107*-Gal-4 (BL #44407)), w^{1118} (BL #5905), UAS:EcRB1 (BL #6469),
508 and Canton S (wild-type) were obtained from Bloomington Stock Center.
509 UAS:Kis.RNAi.a and UAS:Kis.RNAi.b (VDRC #10762 and #46685, respectively) came
510 from the VDRC and were previously described [13]. The kis^{LM27} allele was generated by EMS
511 mutagenesis, as previously described [42]. UAS:Kis-L, Kis-eGFP, *201Y*-Gal-4 MARCM
512 stocks were gifts from J. Tamkun, A. Spralding, and L. Luo, respectively [20,21]. MARCM
513 mosaic analysis clones were generated as previously described [16,43]. The EcR
514 transcriptional reporter (*EcR.1*-Gal-4) was obtained as described [23,24].

515 Pharmacological treatment media was prepared as described [34]. Treated fly media
516 was made using dried instant food (Nutri-Fly Instant, Genesee Scientific) with water
517 containing 1.6% of 10% w/v tegosept (methyl p-hydroxybenzoate in 95% ethanol) and
518 0.1% of DMSO vehicle or 10μM SAHA. *Drosophila* were raised on drug containing food
519 for their entire lifespan.

520

521 Immunohistochemistry

522 Immunohistochemical staining was carried out as previously described [20].
523 Dissections were performed on Sylgard-coated plates in phosphate buffer and fixed in 2%
524 paraformaldehyde. Primary antibodies obtained from the Iowa Developmental Hybridoma
525 Bank included α-EcR-B1 (1:200), α-Gal-4 (1:200), and α-FasII (1:200). Fluorescently
526 conjugated goat α-rabbit or goat α-mouse secondary antibodies (1:100, Jackson
527 Immunoresearch Labs). Brains were mounted in Vectashield with DAPI (Vector
528 Laboratories, H-1000) and images were obtained using an Olympus Fluoview 1000 laser
529 scanning confocal microscope.

530

531 Quantitative RT-PCR

532 Pupal (approximately 18 hours APF) heads or third instar larval brains were
533 dissected in ice-cold phosphate buffer and immediately transferred to RNA Later (Abion)
534 and stored in –80 °C. Isolation of total RNA was done using phenol:chloroform extraction
535 followed by alcohol precipitation for purification. RNA was stored in DEPC water at –80
536 °C. An adapted version of iTaq™ Universal SYBR® Green One-Step protocol (Bio-Rad)
537 was utilized and samples were run on Bio-Rad C1000 Thermal Cycler CFX96 Real-Time
538 system. Primers were made to *Kismet, EcR-B1, Gal-4* mRNAs (IDT). ΔC(t) values were
539 calculated by subtracting the C(t) value of each primer set from C(t) value of *RP49*
540 housekeeping control. Fold change in expression was calculated from ΔΔC(t) values. Each
541 experiment was performed in triplicate with at least three biological replicates.

542

543 Chromatin Immunoprecipitation

544 Brains from third instar larvae were isolated in ice-cold phosphate buffer. Brains
545 were transferred to 1X phosphate buffered saline (PBS, Hyclone) and stored at –80 °C. A
546 modified version of truChIP Tissue Chromatin Shearing Kit with SDS Shearing Buffer
547 protocol (Covaris) was used to shear the DNA. Heads were washed twice with 1X PBS
548 and then fixed in Buffer A with 1% methanol-free formaldehyde for 5 minutes at room
549 temperature. Fixing was stopped with Quenching Buffer E followed by incubation for 5
550 minutes at room temperature. Tissue was pelleted by centrifugation at 4 °C for 5 minutes.
551 Supernatant was removed, and tissue was washed twice with cold 1X PBS. Wash buffer
552 (WB) was removed and tissue was homogenized for 2-3 minutes in 500µL Lysis Buffer
553 (LB) B. Volume was increased to 1mL with LB B followed by incubation on rocker at 4
554 °C for 20 minutes with 3 second vortex every 10 minutes. Lysed tissue was pelleted and
555 resuspened in WB C. Tissue was washed on rocker for 10 minutes at 4°C at which time it
556 was pelleted, followed by an additional washing with WB C without incubation. Pelleted
557 lysed and washed tissue, largely consisting of nuclei, was resuspended in Covaris SDS
558 Shearing Buffer D. The aggregate of nuclei was incubated with Buffer D for 10 minutes
559 with occasional vortex prior to transfer to a TC 12X12 tube for shearing. Shearing followed
560 the S- and E-Series Shearing recommendations for 15 minutes. Aliquots were stored at –
561 80 °C.

562 Sheared DNA was confirmed to be within a target range of 100-600 bp fragments.
563 Chromatin was immunoprecipitated using Magna ChIP™ HiSens kit (Millipore).
564 Antibodies against modifications H3K27me3 (rabbit, ab195477), H3K4me1 (rabbit,
565 ab8895), H3K4me2 (rabbit, ab7766), H3K4me3 (rabbit, ab8580), H3K36me2 (rabbit,
566 ab9049), H3K36me3 (rabbit, ab9050) were used and compared to Histone H3 antibody

567 (rabbit, ab1791). To examine Kismet abundance, α-GFP (rabbit, ab290) was used and α-
568 IgG (rabbit, ab171870) was used as a background control. After elution, samples were
569 incubated with RNaseA (10mg/mL, ThermoScientific) at 37 °C for 30 minutes followed
570 by an incubation with proteinase K (10mg/mL, Millipore) at 57 °C overnight and then
571 inactivate at 75 °C for 15 minutes the next day. Isolated DNA was purified via QIAquick®
572 PCR Purification Kit (Qiagen) and stored at –20 °C.
573
574 MNase Protection Assay
575 Brains from third instar larvae were dissected in ice-cold phosphate buffer,
576 transferred to 1X PBS, and stored at –80 °C. An MNase protection assay was performed
577 using an adapted protocol from [44,45]. Tissue was homogenized in 500µL of crosslinking
578 buffer (60mM KCl, 15mM NaCl, 4mM MgCl2,15mM HEPES pH 7.6, 0.5mM DTT, 0.5%
579 Triton X-100, protease inhibitor (100X), 2% formaldehyde) and incubated at room
580 temperature for 15 minutes. Crosslinking was quenched with 50µL of 2.5M of glycine and
581 incubated at room temperature for 5 minutes. Samples were washed twice in crosslinking
582 buffer and twice in D1 buffer (25% glycerol, 5mM Mg Acetate, 50mM Tris pH 8.0, 0.1mM
583 EDTA, 5mM DTT) and resuspended in 1mL of MNase buffer (60mM KCl, 15mM NaCl,
584 15mM Tris pH 7.4, 0.5mM DTT, 0.25M sucrose, 1.0mM CaCl2). 10units MNase (70196Y,
585 Affymetrix) was added to sample tubes and incubated at 37 °C for 30 minutes. Reaction
586 was quenched with EDTA (final 12.5mM) and SDS (final 0.5%). Samples were
587 equilibrated with NaCl (final 140mM) and incubated with RNaseA (10mg/mL) at 37 °C
588 and then overnight with proteinase K (10mg/mL) at 65 °C and then 15 minutes at 75 °C
589 the next day. DNA was purified via QIAquick PCR Purification Kit and stored at –20 °C.

590

591 Q-PCR

592 Purified DNA was used to prep PCR reaction mixes according to DyNAmo Flash
593 SYBR Green qPCR Kit (ThermoFisher Scientific). Samples were run using Bio-Rad
594 C1000 Thermal Cycler CFX96 Real-Time system. Primers were made to the TSS of *EcR-*
595 *B1*, a 16kb upstream enhancer of *EcR-B1* (*EcR.1*), and a 7.4kb upstream enhancer of *EcR-*
596 *B1* (*EcR.2*) (IDT). Additionally, positive and negative control primers were made to the
597 TSS of *fkh* and the *shi* promoter site, respectively (IDT). For control and RNAi knockdown
598 analysis values were adjusted for input at each primer set and ΔΔC(t) values were
599 calculated by subtracting the adjusted ΔC(t) value of each primer set from the
600 corresponding ΔC(t) IgG control. Fold change in expression was calculated from ΔΔC(t)
601 values. Each experiment was performed in triplicate with at least three biological
602 replicates.

603

604 Behavioral testing

605 To evaluate learning and memory, the canonical fly courtship behavior was used as
606 a readout in an associative conditioning assay described by Siegel and Hall [32]. Virgin male
607 flies (0 to 6 hours following eclosion) were collected in individual food vials and aged 5
608 days. Similarly, virgin female wild-type flies were collected, transferred to collective food
609 vials, and aged 5 days. 24 hours before assessment, virgin wild-type females were mated
610 individually using wild-type males. These flies were subsequently separated from virgin
611 females. This behavioral test was executed in a separate room kept at 25°C and 50%
612 humidity, recorded using a Sony DCR-SR47 Handycam with Carl Zeiss optics, and

613 illuminated from below using a constant 115V white light transilluminator. Genotypes of
614 each male were blinded on the day of the assay and all fly transfers were performed without
615 anesthesia. Aged male flies were transferred to mating chambers (Aktogen) each
616 containing a portioned-off mated female fly. Flies were allowed to acclimate for 2 minutes
617 before the assay. Training was recorded and commenced for 60 minutes. After, the male
618 fly was transferred to a clean mating chamber containing a portioned-off virgin female fly.
619 After an additional 2-minute acclimation period, the divider was removed, and immediate
620 recall was recorded for 10 minutes. Shams experienced the same manipulations however
621 these aged males were not exposed to any fly during the training portion. Digital video
622 analysis of the time spent courting was performed using iMovie software (Apple).
623 Courtship indices were calculated by total time observed performing courtship behaviors
624 divided by total time assayed.
625
626 Statistical analysis
627 All statistical analyses were performed using GraphPad Prism (v. 7.03).
628 Significance was determined at the 95% confidence interval. Unpaired student's *t*-test was
629 used for all experiments, except pupal pruning analysis (utilized one-way ANOVA test)
630 and the learning portion of the associative conditioning assay (utilized paired student's *t*-
631 test). Statistical significance in figures is represented by * = $p < 0.05$, ** = $p < 0.001$, ***
632 = $p < 0.0001$. Error bars represent the standard error of the mean (SEM).
633
634
635
636

Acknowledgements

We would like to thank the members of the Marenda lab for their helpful feedback during the course of this project, the Bloomington Drosophila Stock Center, the Vienna Drosophila Stock Center, and the Developmental Studies Hybridoma Bank for fly stocks, antibodies, and reagents; Drexel CIC for imaging analysis and assistance. We would like to thank J. Tamkun, L. Luo, and A. Spralding for stocks. This work was supported by grants from the CHARGE syndrome Foundation (to D.R.M.) and the National Science Foundation IOS 1256114 (to D.R.M.). Some of this material is based upon work supported by (while serving at) the National Science Foundation. Any opinion, findings, and conclusions or recommendations expressed in this material are those of the author(s) and do not necessarily reflect the views of the National Science Foundation.

660 **References**

661 1 Tau, G. Z. & Peterson, B. S. Normal development of brain circuits.
662 *Neuropsychopharmacology* **35**, 147-168, doi:10.1038/npp.2009.115 (2010).
663 2 Low, L. K. & Cheng, H. J. Axon pruning: an essential step underlying the
664 developmental plasticity of neuronal connections. *Philos Trans R Soc Lond B Biol*
665 *Sci* **361**, 1531-1544, doi:463621T5G6131557 [pii]
666 10.1098/rstb.2006.1883 (2006).
667 3 Awasaki, T., Huang, Y., O'Connor, M. B. & Lee, T. Glia instruct developmental
668 neuronal remodeling through TGF-beta signaling. *Nat Neurosci* **14**, 821-823,
669 doi:10.1038/nn.2833 (2011).
670 4 Yu, F. & Schuldiner, O. Axon and dendrite pruning in Drosophila. *Curr Opin*
671 *Neurobiol* **27**, 192-198, doi:10.1016/j.conb.2014.04.005 (2014).
672 5 Truman, J. W. Metamorphosis of the central nervous system of Drosophila. *J*
673 *Neurobiol* **21**, 1072-1084, doi:10.1002/neu.480210711 (1990).
674 6 Levine, R. B., Morton, D. B. & Restifo, L. L. Remodeling of the insect nervous
675 system. *Curr Opin Neurobiol* **5**, 28-35 (1995).
676 7 Heisenberg, M., Borst, A., Wagner, S. & Byers, D. Drosophila mushroom body
677 mutants are deficient in olfactory learning. *J Neurogenet* **2**, 1-30 (1985).
678 8 Connolly, J. B. *et al.* Associative learning disrupted by impaired Gs signaling in
679 Drosophila mushroom bodies. *Science* **274**, 2104-2107 (1996).
680 9 Ferveur, J. F., Stortkuhl, K. F., Stocker, R. F. & Greenspan, R. J. Genetic
681 feminization of brain structures and changed sexual orientation in male Drosophila.
682 *Science* **267**, 902-905 (1995).
683 10 McBride, S. M. *et al.* Mushroom body ablation impairs short-term memory and
684 long-term memory of courtship conditioning in Drosophila melanogaster. *Neuron*
685 **24**, 967-977, doi:S0896-6273(00)81043-0 [pii] (1999).
686 11 Lee, T., Marticke, S., Sung, C., Robinow, S. & Luo, L. Cell-autonomous
687 requirement of the USP/EcR-B ecdysone receptor for mushroom body neuronal
688 remodeling in Drosophila. *Neuron* **28**, 807-818, doi:S0896-6273(00)00155-0 [pii]
689 (2000).
690 12 Zheng, X. *et al.* TGF-beta signaling activates steroid hormone receptor expression
691 during neuronal remodeling in the Drosophila brain. *Cell* **112**, 303-315,
692 doi:S0092867403000722 [pii] (2003).
693 13 Melicharek, D. J., Ramirez, L. C., Singh, S., Thompson, R. & Marenda, D. R.
694 Kismet/CHD7 regulates axon morphology, memory and locomotion in a
695 Drosophila model of CHARGE syndrome. *Hum Mol Genet* **19**, 4253-4264,
696 doi:ddq348 [pii]
697 10.1093/hmg/ddq348 (2010).
698 14 Layman, W. S., Hurd, E. A. & Martin, D. M. Chromodomain proteins in
699 development: lessons from CHARGE syndrome. *Clin Genet* **78**, 11-20,
700 doi:CGE1446 [pii]
701 10.1111/j.1399-0004.2010.01446.x (2010).
702 15 Vissers, L. E. *et al.* Mutations in a new member of the chromodomain gene family
703 cause CHARGE syndrome. *Nat. Genet.* **36**, 955-957, doi:10.1038/ng1407
704 ng1407 [pii] (2004).

705 16 Lee, T. & Luo, L. Mosaic analysis with a repressible cell marker for studies of gene
706 function in neuronal morphogenesis. *Neuron* **22**, 451-461 (1999).
707 17 Schuldiner, O. *et al.* piggyBac-based mosaic screen identifies a postmitotic
708 function for cohesin in regulating developmental axon pruning. *Dev Cell* **14**, 227-
709 238, doi:S1534-5807(07)00419-4 [pii]
710 10.1016/j.devcel.2007.11.001 (2008).
711 18 Yang, M. Y., Armstrong, J. D., Vilinsky, I., Strausfeld, N. J. & Kaiser, K.
712 Subdivision of the Drosophila mushroom bodies by enhancer-trap expression
713 patterns. *Neuron* **15**, 45-54, doi:0896-6273(95)90063-2 [pii] (1995).
714 19 Boulanger, A. *et al.* ftz-f1 and Hr39 opposing roles on EcR expression during
715 Drosophila mushroom body neuron remodeling. *Nat Neurosci* **14**, 37-44,
716 doi:nn.2700 [pii]
717 10.1038/nn.2700 (2011).
718 20 Ghosh, R. *et al.* Kismet positively regulates glutamate receptor localization and
719 synaptic transmission at the Drosophila neuromuscular junction. *PLoS One* **9**,
720 e113494, doi:10.1371/journal.pone.0113494 (2014).
721 21 Buszczak, M. *et al.* The carnegie protein trap library: a versatile tool for Drosophila
722 developmental studies. *Genetics* **175**, 1505-1531,
723 doi:10.1534/genetics.106.065961 (2007).
724 22 Srinivasan, S., Dorighi, K. M. & Tamkun, J. W. Drosophila Kismet regulates
725 histone H3 lysine 27 methylation and early elongation by RNA polymerase II. *PLoS*
726 *Genet.* **4**, e1000217, doi:10.1371/journal.pgen.1000217 (2008).
727 23 Pfeiffer, B. D. *et al.* Tools for neuroanatomy and neurogenetics in Drosophila.
728 *Proceedings of the National Academy of Sciences of the United States of America*
729 **105**, 9715-9720 (2008).
730 24 Pfeiffer, B. D. *et al.* (2011).
731 25 Clapier, C. R., Iwasa, J., Cairns, B. R. & Peterson, C. L. Mechanisms of action and
732 regulation of ATP-dependent chromatin-remodelling complexes. *Nat Rev Mol Cell*
733 *Biol* **18**, 407-422, doi:10.1038/nrm.2017.26 (2017).
734 26 Dorighi, K. M. & Tamkun, J. W. The trithorax group proteins Kismet and ASH1
735 promote H3K36 dimethylation to counteract Polycomb group repression in
736 Drosophila. *Development* **140**, 4182-4192, doi:10.1242/dev.095786 (2013).
737 27 Stabell, M., Larsson, J., Aalen, R. B. & Lambertsson, A. Drosophila dSet2
738 functions in H3-K36 methylation and is required for development. *Biochem*
739 *Biophys Res Commun* **359**, 784-789, doi:10.1016/j.bbrc.2007.05.189 (2007).
740 28 Wagner, E. J. & Carpenter, P. B. Understanding the language of Lys36 methylation
741 at histone H3. *Nat Rev Mol Cell Biol* **13**, 115-126, doi:10.1038/nrm3274 (2012).
742 29 Bornstein, B. *et al.* Developmental Axon Pruning Requires Destabilization of Cell
743 Adhesion by JNK Signaling. *Neuron* **88**, 926-940,
744 doi:10.1016/j.neuron.2015.10.023 (2015).
745 30 Stewart, B. A. & McLean, J. R. Population density regulates Drosophila synaptic
746 morphology in a Fasciclin-II-dependent manner. *J Neurobiol* **61**, 392-399,
747 doi:10.1002/neu.20096 (2004).
748 31 McBride, S. M. *et al.* Pharmacological rescue of synaptic plasticity, courtship
749 behavior, and mushroom body defects in a Drosophila model of fragile X
750 syndrome. *Neuron* **45**, 753-764, doi:S0896-6273(05)00076-0 [pii]

751 10.1016/j.neuron.2005.01.038 (2005).
752 32 Siegel, R. W. & Hall, J. C. Conditioned responses in courtship behavior of normal
753 and mutant Drosophila. *Proc Natl Acad Sci U S A* **76**, 3430-3434 (1979).
754 33 Siwicki, K. K. *et al.* The role of cuticular pheromones in courtship conditioning of
755 Drosophila males. *Learn Mem* **12**, 636-645, doi:lm.85605 [pii]
756 10.1101/lm.85605 (2005).
757 34 Latcheva, N. K. *et al.* Epigenetic crosstalk: Pharmacological inhibition of HDACs
758 can rescue defective synaptic morphology and neurotransmission phenotypes
759 associated with loss of the chromatin reader Kismet. *Mol Cell Neurosci* **87**, 77-85,
760 doi:10.1016/j.mcn.2017.11.007 (2018).
761 35 Srinivasan, S., Dorighi, K. M. & Tamkun, J. W. Drosophila Kismet regulates
762 histone H3 lysine 27 methylation and early elongation by RNA polymerase II. *PLoS*
763 *Genet* **4**, e1000217, doi:10.1371/journal.pgen.1000217 (2008).
764 36 Srinivasan, S. *et al.* The Drosophila trithorax group protein Kismet facilitates an
765 early step in transcriptional elongation by RNA Polymerase II. *Development* **132**,
766 1623-1635, doi:10.1242/dev.01713 (2005).
767 37 Bell, O. *et al.* Localized H3K36 methylation states define histone H4K16
768 acetylation during transcriptional elongation in Drosophila. *EMBO J* **26**, 4974-
769 4984, doi:10.1038/sj.emboj.7601926 (2007).
770 38 Shogren-Knaak, M. *et al.* Histone H4-K16 acetylation controls chromatin structure
771 and protein interactions. *Science* **311**, 844-847, doi:10.1126/science.1124000
772 (2006).
773 39 Zhang, R., Erler, J. & Langowski, J. Histone Acetylation Regulates Chromatin
774 Accessibility: Role of H4K16 in Inter-nucleosome Interaction. *Biophys J* **112**, 450-
775 459, doi:10.1016/j.bpj.2016.11.015 (2017).
776 40 Barbetti, V. *et al.* Time- and residue-specific differences in histone acetylation
777 induced by VPA and SAHA in AML1/ETO-positive leukemia cells. *Epigenetics* **8**,
778 210-219, doi:10.4161/epi.23538 (2013).
779 41 Brand, A. H. & Perrimon, N. Targeted gene expression as a means of altering cell
780 fates and generating dominant phenotypes. *Development* **118**, 401-415 (1993).
781 42 Melicharek, D. *et al.* Identification of Novel Regulators of Atonal Expression in the
782 Developing Drosophila Retina. *Genetics* **180**, 2095–2110,
783 doi:10.1534/genetics.108.093302 (2008).
784 43 Wu, J. S. & Luo, L. A protocol for mosaic analysis with a repressible cell marker
785 (MARCM) in Drosophila. *Nature protocols* **1**, 2583-2589 (2006).
786 44 Berson, A. *et al.* TDP-43 Promotes Neurodegeneration by Impairing Chromatin
787 Remodeling. *Curr Biol* **27**, 3579-3590 e3576, doi:10.1016/j.cub.2017.10.024
788 (2017).
789 45 Chereji, R. V. *et al.* Genome-wide profiling of nucleosome sensitivity and
790 chromatin accessibility in Drosophila melanogaster. *Nucleic Acids Res* **44**, 1036-
791 1051, doi:10.1093/nar/gkv978 (2016).
792